PHOTONICS Research

Metasurface doublet-integrated bidirectional grating antenna enabling enhanced wavelength-tuned beam steering

Woo-Bin Lee,[1,2] Chul-Soon Im,[2] Changyi Zhou,[1,2] Bishal Bhandari,[1,2] Duk-Yong Choi,[3] and Sang-Shin Lee[1,2,*]

[1]Department of Electronic Engineering, Kwangwoon University, Seoul 01897, Republic of Korea
[2]Nano Device Application Center, Kwangwoon University, Seoul 01897, Republic of Korea
[3]Laser Physics Centre, Research School of Physics, Australian National University, Canberra, ACT 2601, Australia
*Corresponding author: slee@kw.ac.kr

We propose and demonstrate an optical phased-array-based bidirectional grating antenna (BDGA) in silicon nitride waveguides. The BDGA is integrated with a miniaturized all-dielectric metasurface doublet (MD) formed on a glass substrate. The BDGA device, which takes advantage of alternately feeding light to its ports in opposite directions, is presumed to effectively provide a doubled wavelength-tuned steering efficiency compared to its unidirectional counterpart. The MD, which is based on vertically cascaded convex and concave metalenses comprising circular hydrogenated amorphous silicon nanopillars, is meticulously placed atop the BDGA chip to accept and deflect a beam emanating from the emission area, thereby boosting the beam-steering performance. The manufactured BDGA could achieve an enhanced beam-steering efficiency of 0.148 deg/nm as well as a stable spectral emission response in the wavelength range of 1530–1600 nm. By deploying a fabricated MD atop the silicon photonic BDGA chip, the steering efficiency was confirmed to be boosted by a factor of ∼3.1, reaching 0.461 deg/nm, as intended. © 2021 Chinese Laser Press

1. INTRODUCTION

Optical phased array (OPA) is widely perceived as an outstanding beam-steering strategy owing to its salient advantages that include a low divergent beam, flexible 2D beamforming, and ultrafast inertia-free steering [1–6]. Integrated-circuit type OPAs, which are a prominent candidate for light detection and ranging (lidar), have attracted immense interest for applications such as sensing, 3D mapping, navigation for self-driving cars, and autonomous drones [7–11]. However, solid-state beam steering suffers from a narrower field of view than mechanical methods such as a micro–electromechanical system (MEMS) mirror, gimbal, and prism [12–14]. The scanning span along the longitudinal direction of an OPA is determined by the wavelength tuning range of the light source as well as the diffraction grating constituting the OPA. A waveguide diffraction grating delivers a typically small angular dispersion of below 0.140 deg/nm [15]. Thus, a broadband tunable laser with a tuning range exceeding 100 nm was used to expand the steering range [1,15–19]. However, a widely tunable laser is extremely difficult to embody and requires complex control schemes to access all wavelengths [20,21]. The beam-steering range in

the longitudinal direction should be addressed to overcome the inherent limitations of OPA-based emitters.

Recently, various configurations of lenses and prisms, which are used to manipulate a beam in free space, have been devised to execute wide-angle beam steering by amplifying the steering efficiency [15,22–24]. These methods are known for demonstrating wide-angle steering, but require bulky components and mounting fixtures with dimensions of several centimeters. Compared to the bulky lens systems, a metasurface device, featuring an ultrathin, flat form factor, can be engineered to provide high design flexibility [25–28]. Studies have attempted to directly integrate such metasurfaces into a silicon photonic circuit to contrive compact beam manipulations in terms of emission positions and radiation modes [25,29]. Nonetheless, a common monolayer metasurface may be limited in increasing the field of view of an OPA [25,30,31]. In this context, the steering efficiency (deg/nm) of the OPA, determined by an angular shift in response to a wavelength tuning, can be enhanced significantly by relying on a metasurface doublet (MD), as reported in our previous work [31]. To date, to the best of our knowledge, no studies have reported research on an MD in conjunction with a silicon photonic bidirectional grating

antenna (BDGA) to efficiently enhance the beam steering efficiency.

This work presents a BDGA that incorporates an MD featuring a flat and ultrathin form factor for efficient beam steering. Compared to conventional grating antennas, the BDGA, which is capable of bidirectional beam steering, effectively imparts twice the steering range within a given wavelength-tuning range. The steering performance of the BDGA, which emits light in a vertical direction, is characterized in terms of the steering range and spectral emission response of the main beam along the longitudinal direction. Furthermore, the MD, operating as a steering angle magnifying metalens is integrated into the BDGA to amplify threefold the wavelength-tuned steering efficiency. The ultrathin and polarization-insensitive MD that constitutes two disparate metasurfaces enables relatively straightforward alignment with the silicon photonic circuit for performance improvement. Finally, the emission response of the MD-integrated BDGA is analyzed after evaluating the transfer characteristic of the MD. We believe this approach provides a functional flat form factor to realize an OPA with high beam-steering efficiency.

2. DESIGN OF THE PROPOSED BDGA AND MD TO BOOST THE BEAM-STEERING EFFICIENCY

The narrow beam-steering range in a nonmechanical system can be dramatically extended by resorting to lens optics [22,23]. This approach can be similarly applied to enhance the steering performance of an OPA to substantially expand the achievable scanning range under a given wavelength-tuning range. Figure 1 depicts the schematic configuration of the proposed scheme, in which an MD is incorporated atop a BDGA to further enhance the beam steering. The BDGA chip in silicon is configured so that light is launched through a spot size converter and split into five stages of 1 × 2 multimode interference couplers, prior to impinging upon a set of waveguide grating channels. A light beam is ultimately radiated from the surface-relief gratings comprising the 32-channel BDGA. The proposed platform taps into a variable ratio coupler, which plays the role of alternating the light path between Ports 1 and 2, thereby doubling the scanning range of the optical antenna. The achievable steering range $\Delta\theta$ hinges on the

wavelength-tuning range, from λ_1 to λ_2, of the light source. The light is presumed to radiate vertically in the case of λ_1, and it progressively inclines in the backward direction with increasing wavelengths. The beam emanating from the antenna impinges upon the MD aligned directly above it, which is deemed to deflect the incoming beam by a factor of M. The beam steering can be ultimately amplified with the help of the MD, featuring a compact footprint unlike conventional bulky lens optics.

A. Proposed BDGA Enabling Bidirectional Beam Emission

Figure 2(a) illustrates a schematic of the suggested BDGA and its principle of operation. Silicon nitride (SiN) is used for the waveguide core because of its advantages of a broad transparency window, low loss, and conspicuous fabrication reliability [32–34]. A SiN waveguide with a thickness (h_{SiN}) of 450 nm was deposited through low-pressure chemical vapor deposition on top of a buried oxide (BOX) layer with a thickness (h_{BOX}) of 4 μm laid on a silicon substrate. The waveguide was patterned using a deep ultraviolet (DUV) stepper to achieve a 2 μm width, and it was subsequently partially etched to create a grating according to a groove height of 90 nm. The 32-channel BDGA appended with the cascaded MMI splitters was designed to have a uniform spacing of 4 μm. Finally, the SiN waveguide patterns were covered with a 3 μm thick oxide cladding, thus protecting them from damage.

Unlike conventional grating counterparts, the proposed BDGA can support bidirectional beam radiation by alternately feeding light to the two ports. The emission angle θ is formulated as $\sin\theta(\lambda) = n_{eff} - \lambda/\Lambda$, where n_{eff} is the effective refractive index of the grating waveguide and Λ is the grating period. The beam should be normally emitted ($\theta = 0°$) for the shortest wavelength of the given tuning range, so that continuous beam scanning can be conducted by alternating the light launching port. Under a fixed wavelength-tuning span, the BDGA achieves a beam-steering range of $-\Delta\theta(\lambda)$ and $\Delta\theta(\lambda)$ in the backward direction for Ports 1 and 2, respectively. This implies that the scanning range can be effectively expanded twofold. It is noteworthy that the backward emission, invoked by a strong grating vector, leads to a higher steering efficiency than the forward emission [35].
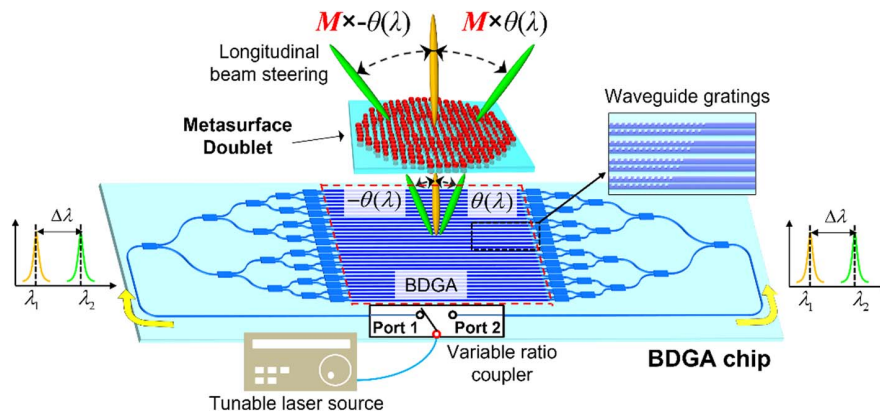

Fig. 1. Schematic configuration of the proposed BDGA incorporating an MD, enabling an enhanced beam-steering efficiency in the longitudinal direction.
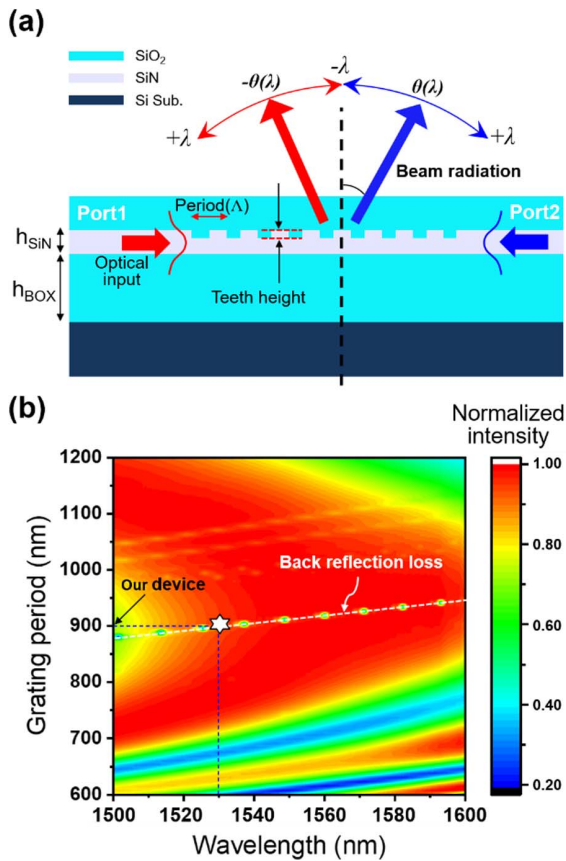
(a)

(b)

Fig. 2. (a) Configuration of the proposed BDGA and its operation that extends the beam-steering range. (b) Calculated spectral emission response with respect to the grating period for a 2D modeled BDGA for $h_{BOX} = 4 \ \mu m$.

For a 2D modeled SiN antenna, as illustrated in Fig. 2(b), the emission spectra are numerically designed to radiate the beam normally with the assistance of Lumerical FDTD Solutions (Ansys Lumerical). A 500 μm long SiN waveguide incorporates a partially etched surface grating, with a fill factor of 0.5 and a height of 90 nm. The effective refractive index of the waveguide was calculated as ~1.69 at $\lambda = 1550$ nm. Figure 2(b) shows that the optical intensity for the vertical out-coupling corresponding to $\theta = 0°$ drops in response to the grating period. Back reflection corresponding to the second-order diffraction that pertains to the waveguide gratings diminishes the upward radiation along the dotted white line [18]. Under the given spectral range of 1530–1600 nm, the grating period was set to 900 nm to perform continuous bidirectional beam scanning. The spectral emission response has been reported to be critically affected by the thickness of the BOX layer, which operates as a cavity [36]. To sidestep the resonance dip that incurs a degradation in upward emission intensity, a 4 μm thick BOX was primarily adopted to exhibit a consistent spectral emission response. A BDGA structure leading to the vertical emission is preferred from the standpoint of deploying a lens to amplify the steering range. An off-vertical beam requires a sophisticated off-axis mounting strategy and occupies much volume. Considering that the space pertaining to the tilt between the beam and lens optics engenders an enlarged beam, the lens should be accordingly increased in size. However, the proposed BDGA, operating as a vertical radiator, is expected to preferentially amplify the steering range under a compact form factor.

B. MD as a Steering Angle Magnifying Metalens

Figure 3(a) describes the concept of an ultrathin lens system that taps into the MD to increase the steering efficiency. Here, the MD comprises a glass substrate with a thickness of 902 μm, sandwiched between metasurface 1 (MS1) and metasurface 2 (MS2), which function as convex and concave lenses, respectively. MS1 and MS2 comprise circular nanopillars in hydrogenated amorphous silicon (a-Si:H), with heights of 880 nm. The simulated magnetic field is displayed for a-Si:H nanopillars, showing that the field is strongly confined inside the nanopillar. By regulating the diameters of the pillars from 200 to 494 nm, the incident light was manipulated to sufficiently undergo a phase shift covering a span of 0 to 2π. The incident beam converges inwardly via MS1 and then deflects outwardly through MS2, thus boosting the beam steering. The magnification factor M for the beam deflection is governed by the ratio of the focal lengths of the two meta-surfaces. The focal lengths of MS1 (f_{MS1}) and MS2 (f_{MS2}) are 0.986 and 0.329 mm, respectively, rendering an approximately threefold magnification. When the distance between the BDGA and MD was within 1 mm, the beam emerging from the BDGA was mostly accommodated via an MD with
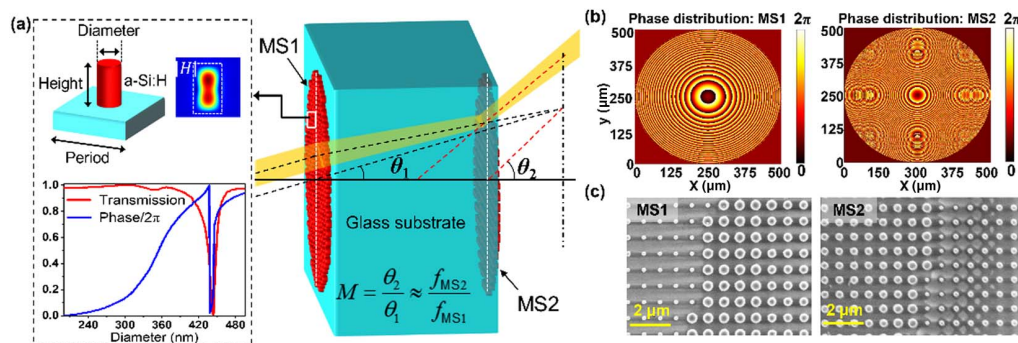

Fig. 3. (a) Configuration of the proposed MD, comprising MS1 and MS2, facilitating the magnification of the beam-steering range. A meta-atom (or unit cell) and the highly confined magnetic field are also included. (b) Designed phase profile of the MD and (c) SEM images of the fabricated MS1 and MS2.

a diameter of 500 μm. The beam going through the MD was steered to assume triple the angle of incidence. The proposed MD can operate independently of the incident polarization owing to its geometrically symmetric structure [37,38]. The phase profile is derived and relocated to obtain circular symmetry, as illustrated in Fig. 3(b). The phase profiles of the geometrical lens to model MS1 and MS2 are expressed by $\varphi_{MS1}(x,y) = \frac{2\pi n}{\lambda} \frac{0.29(x^2+y^2)}{1+\sqrt{1+3.1\times(0.29)^2(x^2+y^2)}}$ and $\varphi_{MS2}(x,y) = \frac{2\pi n}{\lambda} \frac{0.87(x^2+y^2)}{1+\sqrt{1-(0.87)^2(x^2+y^2)}}$, respectively, where n is the refractive index of the modeled lens and λ is the operating wavelength. The derivation and calculation of the phase profiles are provided in detail in Ref. [31]. Figure 3(c) reveals scanning electron microscope images of the proposed MD, signaling that the metasurfaces were faithfully manufactured according to the previously reported process [31].

3. RESULTS AND DISCUSSIONS

A. Characterization of the Fabricated BDGA

Figure 4(a) presents the test setup to evaluate the beam-steering efficiency of the proposed BDGA. A tunable laser (Santec Corp., TLS-210) serves as a light source to provide a wide range of wavelengths between 1530 and 1600 nm. Light was directed to a variable ratio coupler (KS Photonics Inc.) through an erbium-doped fiber amplifier. To fulfill selective optical feeding to the two ports of the BDGA, we used a coupler instead of a 1 × 2 optical switch. A polarization controller (KS Photonics) was deployed at each port to provide incident transverse electric polarized light, which is ultimately edge-coupled to the BDGA via a lensed fiber. Accordingly, the grating antenna emits a light into free space. The main beam component of the light is primarily captured by a beam profiler (CINOGY Technologies GmbH, CMOS-1202). As shown in Fig. 4(b), a well-defined beam is obtained and exhibits FWHM divergence angles of

0.6° and 0.2° along the transverse and longitudinal directions, respectively. The emission angle was measured using the beam profiler, as shown in Fig. 4(c). Considering that the BDGA is designed to assume a strong grating vector for boosting the beam-steering efficiency, the beam was radiated backward, opposite to the launching direction through either Port 1 or 2. As a result, the beam was scanned between +5.4° and –5.4° in response to wavelengths varying from 1530 to 1600 nm. Fabrication errors incurred a slight unexpected offset of 0.2° to the angle of the main beam. The achieved steering efficiency of 0.148 deg/nm is double that of a unidirectional case as intended, showing superiority over the efficiency of the recently reported backward-emitting SiN antenna [35]. The bidirectional beam scanning was executed by switching between Ports 1 and 2 for light launching. For the proposed BDGA, the footprint of the MD may be judiciously miniaturized by dwindling the gap between the grating chip and MD, while safely accommodating the radiated beam.

Figure 5 shows the beam emission efficiency corresponding to the main beam for a wavelength of 1530–1600 nm. The efficiency declined slightly with increasing wavelengths owing to the presence of a resonance dip, which was forged at longer wavelengths [36], resulting in a variation of ~4 dB over a wavelength span of 70 nm. Therefore, the extension of the wavelength-tuning range to broaden the angular scanning may be inevitably limited owing to the degradation in efficiency in response to the increasing wavelengths. However, when using the BDGA, this problem can be effectively circumvented by alternating the launching port, thereby attaining a beam-scanning range of ~10° under an efficiency variation below 4 dB. Consequently, it is categorically claimed that the proposed BDGA is superior to its unidirectional counterpart in terms of the beam-steering efficiency and the spectral emission response.
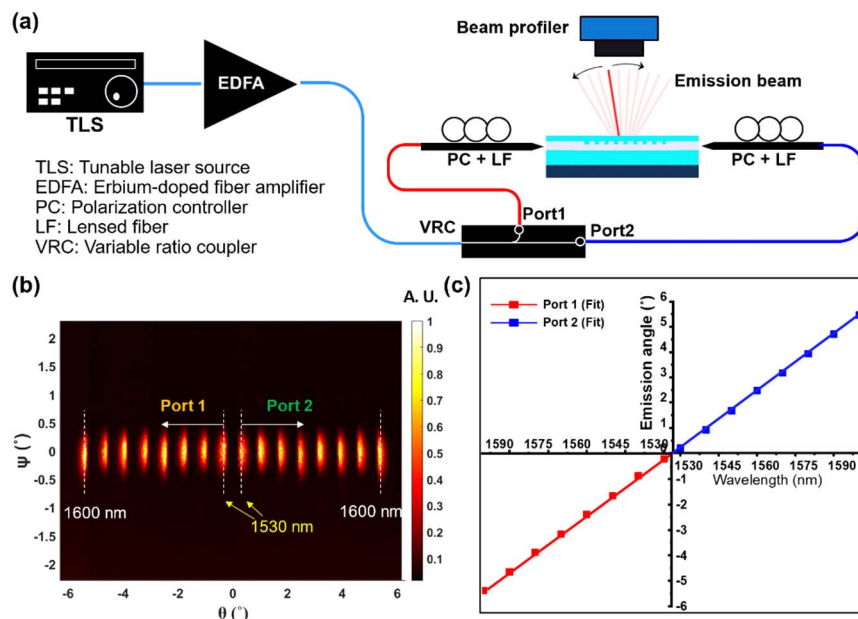

Fig. 4. (a) Experimental setup to inspect the performance of the prepared BDGA. (b) Captured intensity profiles of the wavelength-tuned main beam. (c) Observed emission angles corresponding to the main beam in terms of the wavelength.
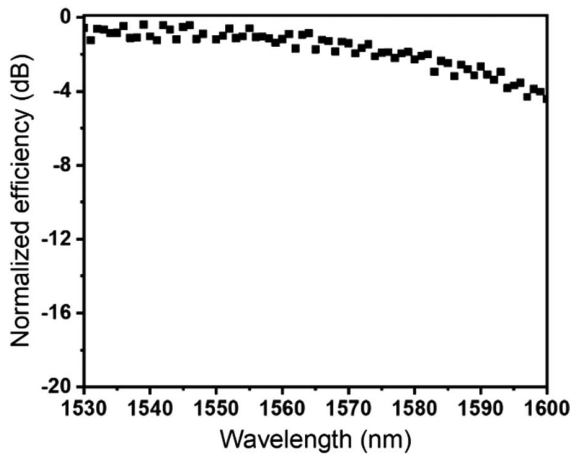
Fig. 5. Measured emission efficiency of the main beam versus the wavelength.

B. Deflection and Transmission Characteristics of the MD

We experimentally investigated the optical response of the MD before its incorporation into the BDGA, as delineated in Fig. 6(a). A collimated beam is polarized and directed toward the MD via a pinhole, with a diameter of 300 μm, to constrict the beam size. The deflected beam emerging from the MD was monitored using a beam profiler. Figure 6(b) shows the angle (θ_d) and efficiency of deflection as a function of the incident angle (θ_i). The measured magnification factor M, given by θ_d/θ_i, corresponds to the calculated value of 3. Indeed, we examined the simulated and measured maximum incident angle for the proposed MD. When light is allowed to pass through MS1 and MS2 that constitute the MD, the angle of incidence at which the MD operates as intended is limited to 14°. For angles exceeding the maximum angle, incident light is deflected along an unexpected direction, which may be attributed to the spherical aberration and off-axis illumination [30]. The deflection efficiency, defined as the ratio of the deflected optical power to the input optical power, reaches 40% and tends to decline with an increasing angle, which might stem from the increased reflection, absorption, scattering, and light leaking in relation to MS1 and MS2 [31]. As shown in Fig. 6(c), the power of the deflected beam weakens with the incident angle, while the beam that is not deflected is concurrently observable as displayed in the inset. The deflection efficiency is surely aggravated as the portion of the undeflected beam power increases. The extinction ratio of the deflected beam with respect to the incident polarization is below 0.3 dB, indicating the MD performance is decently preserved, regardless of the rotational alignment of the MD mounted atop the BDGA. In addition, a broad working wavelength range corresponding to 1500–1600 nm was achieved in our previous work [31], where the deflected beam exhibited a negligible angular shift. The MD is highly anticipated to serve as a steering angle magnifying metalens, featuring a wavelength tuning range of 70 nm.

C. Evaluation of the BDGA Incorporating the MD

Figure 7(a) shows microscopic images of the top and side views of the BDGA combined with the MD. The substrate of the MD is placed squarely above the BDGA chip, which is fixed by a holder. The gap between the BDGA and MD is meticulously adjusted to be below 1 mm through an *XYZ* translation stage. The tilt error of the MD, which may distort the beam profile and induce an angular offset, has been effectively prevented. Light is alternately launched toward Ports 1 and 2 of the BDGA, and the beam emanating from the BDGA is deliberately deflected by the MD mounted atop it. Figure 7(b) illustrates the observed main beam profiles of the BDGA and the BDGA integrated with the MD, as projected on a beam profiler
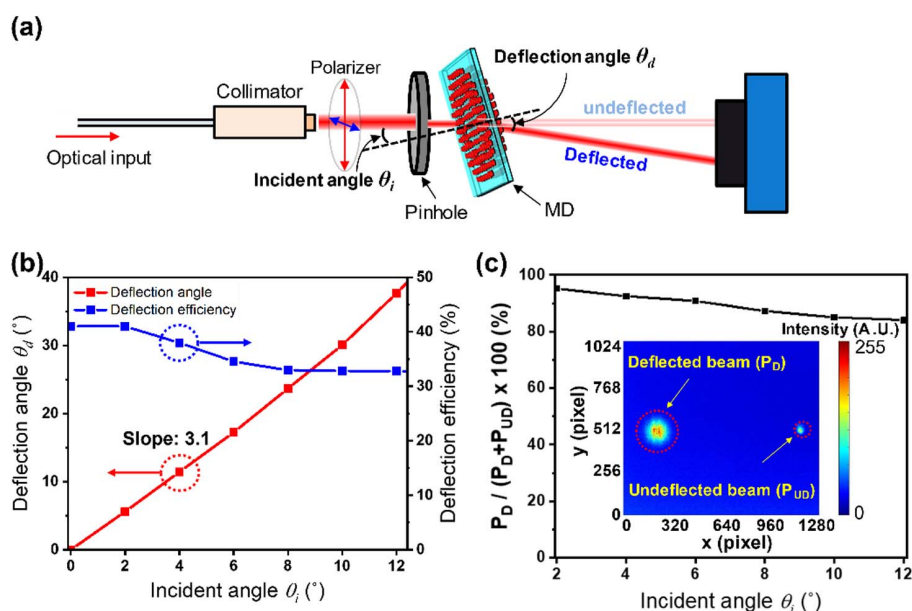

Fig. 6. (a) Test setup to examine the beam deflection based on the MD with the incident angle. (b) Measured deflection angle and deflection efficiency. (c) Relative deflected beam power as a function of the incident angle.
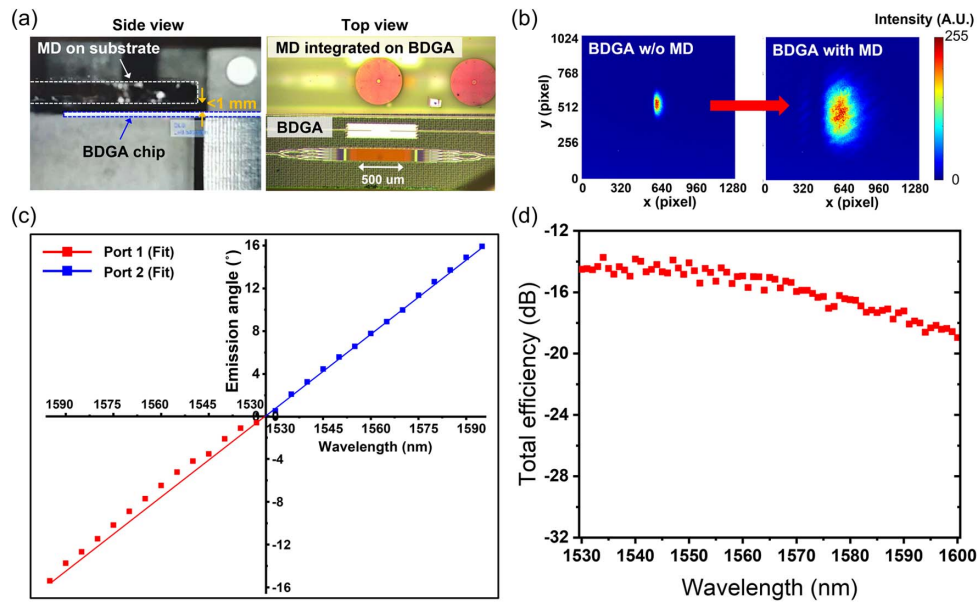
Fig. 7. (a) Side and top views of the BDGA integrated with the MD. (b) Captured intensity profiles of the main beam radiated from BDGA without and with the MD. (c) Measured beam emission angle versus the wavelength. (d) Measured total efficiency of the main beam deflected by the MD versus the wavelength.

at the same distance. The MD is deemed to expand the size of the main beam, whose divergence is tripled to assume 1.8° and 0.7° along the transverse and longitudinal directions, respectively. The beam divergence was correspondingly enlarged three times omnidirectionally, which might possibly deteriorate the angular resolution. This problem may be mitigated by increasing the number of grating antenna elements to enlarge the aperture [2]. The transfer characteristics of the MD-integrated BDGA were scrutinized in terms of the steering angle in the wavelength range of 1530 and 1595 nm, as shown in Fig. 7(c). When the angular range of the beam impinging upon the MD was ±4.9°, the resulting steering range of the outgoing beam was amplified to be ±15°. Thus, the steering efficiency was boosted threefold with the use of the MD as intended, equivalent to 0.461 deg/nm. It is noteworthy that there is a discrepancy in the angular positions of the observed beam spots, as compared to the expected emission angles of the BDGA, which is likely ascribed to misalignment between the BDGA and MD. We verified that the proposed MD is useful for ameliorating the beam-steering efficiency of a silicon photonic device such as the manufactured BDGA. For the MD-incorporated BDGA, the emitted beam can be readily steered over a longitudinal range of 30°. Magnification factor M of the MD, currently set as 3, can be elevated to a certain extent that the appropriate light interaction is secured.

We have explored the optical throughput of the main beam, emerging from the MD, by monitoring the corresponding power captured by the receiving photodiode (Thorlabs, S132C), inclusive of the coupling associated with the spot size converter, as shown in Fig. 7(d). The total efficiency was observed to vary between –14 dB and –19 dB over a wavelength range of 1530–1600 nm. Currently, the proposed device may not be practically applied to fulfill a long-distance scanning,

considering the beam divergence as well as the optical loss should be improved. In fact, the aperture of the beam emitter must be enlarged to reduce the beam divergence, while the insertion loss should be curtailed by optimizing the MD. Moreover, the current device, in which an external variable ratio coupler is used to selectively feed light to the ports of the BDGA, is disadvantageous in terms of integration and operation speed. From the perspective of miniaturizing the proposed MD-based BDGA and fulfilling wide-angle 2D beam scanning, a monolithic switching element may be implemented based on a microheater rendering a thermal phase shift.

4. CONCLUSION

We demonstrated highly efficient beam steering with a BDGA incorporating an MD. The steering efficiency of the proposed BDGA was obtained as approximately 0.148 deg/nm, which was doubled by bidirectionally feeding the light. The structure of the BDGA provided stability to the emission spectral response and enabled vertical radiation, ensuring its suitability for magnifying steering angle devices. An ultrathin, polarization-insensitive MD amplifying the angle of beam steering was used to enhance the steering efficiency of the nonmechanical beam scanner. The implemented MD, which increased the steering efficiency threefold, was mounted on top of the BDGA, thereby expanding its steering range. We verified that our platform improves the steering performance, and had a compact form factor compared to that of conventional bulky lens systems. Finally, the wavelength-tuned steering efficiency was 0.461 deg/nm, which represents a threefold increase over a conventional grating antenna within a given wavelength-tuning range. The proposed approach, which greatly enhances beam-steering efficiency while minimizing space consumption,

could facilitate the development of practical solid-state beam steering.

Disclosures. The authors declare no conflicts of interest.

Data Availability. Data underlying the results presented in this paper are not publicly available at this time but may be obtained from the authors upon reasonable request.

REFERENCES

1. D. N. Hutchison, J. Sun, J. K. Doylend, R. Kumar, J. Heck, W. Kim, C. T. Phare, A. Feshali, and H. Rong, "High-resolution aliasing-free optical beam steering," Optica **3**, 887–890 (2016).
2. M. R. Kossey, C. Rizk, and A. C. Foster, "End-fire silicon optical phased array with half-wavelength spacing," APL Photon. **3**, 011301 (2018).
3. W. Xu, L. Zhou, L. Lu, and J. Chen, "Aliasing-free optical phased array beam-steering with a plateau envelope," Opt. Express **27**, 3354–3368 (2019).
4. J. Sun, E. Timurdogan, A. Yaacobi, E. S. Hosseini, and M. R. Watts, "Large-scale nanophotonic phased array," Nature **493**, 195–199 (2013).
5. W. Guo, P. R. A. Binetti, C. Althouse, M. L. Mašanović, H. P. M. M. Ambrosius, L. A. Johansson, and L. A. Coldren, "Two-dimensional optical beam steering with InP-based photonic integrated circuits," IEEE J. Sel. Top. Quantum Electron. **19**, 6100212 (2013).
6. J. C. Hulme, J. K. Doylend, M. J. R. Heck, J. D. Peters, M. L. Davenport, J. T. Bovington, L. A. Coldren, and J. E. Bowers, "Fully integrated hybrid silicon two dimensional beam scanner," Opt. Express **23**, 5861–5874 (2015).
7. C.-P. Hsu, B. Li, B. Solano-Rivas, A. R. Gohil, P. H. Chan, A. D. Moore, and V. Donzella, "A review of and perspective on optical phased array for automotive LiDAR," IEEE J. Sel. Top. Quantum Electron. **27**, 8300416 (2021).
8. S. A. Miller, C. T. Phare, Y.-C. Chang, X. Ji, O. A. J. Gordillo, A. Mohanty, S. P. Roberts, M. C. Shin, B. Stern, M. Zadka, and M. Lipson, "512-element actively steered silicon phased array for low-power LIDAR," in *Conference on Lasers and Electro-Optics (CLEO)* (OSA, 2018), paper JTh5C.2.
9. C. V. Poulton, "Integrated LIDAR with optical phased arrays in silicon photonics," M.S. dissertation (Massachusetts Institute of Technology, 2016).
10. S. Chung, H. Abediasl, and H. Hashemi, "A monolithically integrated large-scale optical phased array in silicon-on-insulator CMOS," IEEE J. Solid-State Circuits **53**, 275–296 (2018).
11. F. Aflatouni, B. Abiri, A. Rekhi, and A. Hajimiri, "Nanophotonic projection system," Opt. Express **23**, 21012–21022 (2015).
12. M. Zadka, Y.-C. Chang, A. Mohanty, C. T. Phare, S. P. Roberts, and M. Lipson, "On-chip platform for a phased array with minimal beam divergence and wide field-of-view," Opt. Express **26**, 2528–2534 (2018).
13. P. F. Van Kessel, L. J. Hornbeck, R. E. Meier, and M. R. Douglass, "A MEMS-based projection display," Proc. IEEE **86**, 1687–1704 (1998).
14. W. S. Rabinovich, C. I. Moore, R. Mahon, P. G. Goetz, H. R. Burris, M. S. Ferraro, J. L. Murphy, L. M. Thomas, G. C. Gilbreath, M. Vilcheck, and M. R. Suite, "Free-space optical communications

15. H. Ito, Y. Kusunoki, J. Maeda, D. Akiyama, N. Kodama, H. Abe, R. Tetsuya, and T. Baba, "Wide beam steering by slow-light waveguide gratings and a prism lens," Optica **7**, 47–52 (2020).
16. J. K. Doylend, M. J. R. Heck, J. T. Bovington, J. D. Peters, L. A. Coldren, and J. E. Bowers, "Two-dimensional free-space beam steering with an optical phased array on silicon-on-insulator," Opt. Express **19**, 21595–21604 (2011).
17. D. Kwong, A. Hosseini, J. Covey, Y. Zhang, X. Xu, H. Subbaraman, and R. T. Chen, "On-chip silicon optical phased array for two-dimensional beam steering," Opt. Lett. **39**, 941–944 (2014).
18. K. V. Acoleyen, W. Bogaerts, J. Jágerská, N. Le Thomas, R. Houdré, and R. Baets, "Off-chip beam steering with a one-dimensional optical phased array on silicon-on-insulator," Opt. Lett. **34**, 1477–1479 (2009).
19. Y. Zhu, S. Zeng, and L. Zhu, "Optical beam steering by using tunable, narrow-linewidth butt-coupled hybrid lasers in a silicon nitride photonics platform," Photon. Res. **8**, 375–380 (2020).
20. S. Matsuo and T. Segawa, "Microring-resonator-based widely tunable lasers," IEEE J. Sel. Top. Quantum Electron. **15**, 545–553 (2009).
21. G.-L. Su and M. C. Wu, "Widely tunable semiconductor lasers with three interferometric arms," Opt. Express **25**, 21400–21409 (2017).
22. M. Zohrabi, R. H. Cormack, and J. T. Gopinath, "Wide-angle nonmechanical beam steering using liquid lenses," Opt. Express **24**, 23798–23809 (2016).
23. M. Zohrabi, W. Y. Lim, R. H. Cormack, O. D. Supekar, V. M. Bright, and J. T. Gopinath, "Lidar system with nonmechanical electrowetting-based wide-angle beam steering," Opt. Express **27**, 4404–4415 (2019).
24. C.-S. Im, S.-M. Kim, K.-P. Lee, S.-H. Ju, J.-H. Hong, S.-W. Yoon, T. Kim, E.-S. Lee, B. Bhandari, C. Zhou, S.-Y. Ko, Y.-H. Kim, M.-C. Oh, and S.-S. Lee, "Hybrid integrated silicon nitride–polymer optical phased array enabling efficient light detection and ranging," J. Lightwave Technol. **39**, 4402–4409 (2021).
25. Y.-C. Chang, M. C. Shin, C. T. Phare, S. A. Miller, E. Shim, and M. Lipson, "2D beam steerer based on metalens on silicon photonics," Opt. Express **29**, 854–864 (2021).
26. L. Jin, Z. Dong, S. Mei, Y. F. Yu, Z. Wei, Z. Pan, S. D. Rezaei, X. Li, A. I. Kuznetsov, Y. S. Kivshar, J. K. W. Yang, and C.-W. Qiu, "Noninterleaved metasurface for (2⁶−1) spin- and wavelength-encoded holograms," Nano Lett. **18**, 8016–8024 (2018).
27. M. Khorasaninejad, W. T. Chen, R. C. Devlin, J. Oh, A. Y. Zhu, and F. Capasso, "Metalenses at visible wavelengths: diffraction-limited focusing and subwavelength resolution imaging," Science **352**, 1190–1194 (2016).
28. L. Jin, Y.-W. Huang, Z. Jin, R. C. Devlin, Z. Dong, S. Mei, M. Jiang, W. T. Cheng, Z. Wei, H. Liu, J. Teng, A. Danner, X. Li, S. Xiao, S. Zhang, C. Yu, J. K. W. Yang, F. Capasso, and C.-W. Qiu, "Dielectric multi-momentum meta-transfer in the visible," Nat. Commun. **10**, 4789 (2019).
29. A. Yulaev, W. Zhu, C. Zhang, D. A. Westly, H. J. Lezec, A. Agrawal, and V. Aksyuk, "Metasurface-integrated photonic platform for versatile free-space beam projection with polarization control," ACS Photon. **6**, 2902–2909 (2019).
30. A. Arbabi, E. Arbabi, S. M. Kamali, Y. Horie, S. Han, and A. Faraon, "Miniature optical planar camera based on a wide-angle metasurface doublet corrected for monochromatic aberrations," Nat. Commun. **7**, 13682 (2016).
31. C. Zhou, W.-B. Lee, C.-S. Park, S. Gao, D.-Y. Choi, and S.-S. Lee, "Multifunctional beam manipulation at telecommunication wavelengths enabled by an all-dielectric metasurface doublet," Adv. Opt. Mater. **8**, 2000645 (2020).
32. A. Rahim, E. Ryckeboer, A. Z. Subramanian, S. Clemmen, B. Kuyken, A. Dhakal, A. Raza, A. Hermans, M. Muneeb, S. Dhoore, Y. Li, U. Dave, P. Bienstman, N. L. Thomas, G. Roelkens, D. V. Thourhout, P. Helin, S. Severi, X. Rottenberg, and R. Baets, "Expanding the silicon photonics portfolio with silicon nitride photonic integrated circuits," J. Lightwave Technol. **35**, 639–649 (2017).

research and demonstrations at the U.S. Naval Research Laboratory," Appl. Opt. **54**, F189–F200 (2015).

33. D. J. Moss, R. Morandotti, A. L. Gaeta, and M. Lipson, "New CMOS-compatible platforms based on silicon nitride and Hydex for nonlinear optics," Nat. Photonics **7**, 597–607 (2013).

34. P. Muñoz, G. Micó, L. A. Bru, D. Pastor, D. Pérez, J. D. Doménech, J. Fernández, R. Baños, B. Gargallo, R. Alemany, A. M. Sánchez, J. M. Cirera, R. Mas, and C. Domínguez, "Silicon nitride photonic integration platforms for visible, near-infrared and mid-infrared application," Sensors **17**, 2088 (2017).

35. C.-S. Im, B. Bhandari, S.-M. Kim, M.-C. Oh, K.-P. Lee, T. Kim, and S.-S. Lee, "Backward-emitting silicon nitride optical phased array enabling efficient wavelength-tuned beam steering," IEEE Photon. J. **12**, 6601910 (2020).

36. C.-S. Im, B. Bhandari, K.-P. Lee, S.-M. Kim, M.-C. Oh, and S.-S. Lee, "Silicon nitride optical phased array based on a grating antenna enabling wavelength-tuned beam steering," Opt. Express **28**, 3270–3279 (2020).

37. D. Lee, J. G. Hwang, D. Lim, T. Hara, and S. Lim, "Incident angle- and polarization-insensitive metamaterial absorber using circular sectors," Sci. Rep. **6**, 27155 (2016).

38. N. Mahmood, I. Kim, M. Q. Mehmood, H. Jeong, A. Akbar, D. Lee, M. Saleem, M. Zubair, M. S. Anwar, F. A. Tahir, and J. Rho, "Polarisation insensitive multifunctional metasurfaces based on all-dielectric nanowaveguides," Nanoscale **10**, 18323–18330 (2018).